Zhou et al. *Zool. Res. Divers. Conserv.* 2025, 2(3): 182−193
https://doi.org/10.24272/j.issn.2097-3772.2025.025
https://cstr.cn/32249.14.zrdc.2025.025

ZRDC | Zoological Research: Diversity and Conservation

Article Open Access

Dietary niche partitioning among threatened ungulates in the desert ecosystems of northwestern China

Zhi-Chao Zhou[1], Jin Shang[1], De-Feng Chen[1], Li-Na Yi[1], Chang-Liang Shao[2], Dong Zhang[1,*], De-Fu Hu[1,*]

[1] *School of Ecology and Nature Conservation*, *Beijing Forestry University*, *Beijing* 100083, *China*
[2] *Kalamaili Nature Reserve*, *Urumqi* 830000, *China*

ABSTRACT

In arid desert environments where resources are scarce, the mechanisms enabling stable coexistence among sympatric large ungulates remain poorly understood. To address this, fecal DNA metabarcoding was employed to assess dietary niche partitioning among three threatened species —Przewalski's horse (PH; *Equus ferus przewalskii*), Asiatic wild ass (AWA; *Equus hemionus*), and goitered gazelle (GG; *Gazella subgutturosa*) —within the Kalamaili Nature Reserve, a critical hotspot for desert ungulates in China. Results revealed that the two equid species exhibited generalist feeding strategies, while GGs displayed dietary specialization. No clear trophic segregation was observed between reintroduced PHs and native species, indicating incomplete niche differentiation. Significant positive correlations were identified between dietary dissimilarity and geographic separation for both AWAs and GGs, with the GG diet showing greater geographic sensitivity. The native species demonstrated patch-specific dietary shifts, suggesting resource partitioning in response to environmental heterogeneity. The complementary use of spatially distinct resource patches reduced direct competition, thereby facilitating long-term, stable coexistence. However, patches with intermediate niche overlap showed the highest competition intensity, highlighting these transitional zones as critical targets for conservation. These findings provide a theoretical foundation for assessing the viability of reintroduced populations and guiding conservation strategies for threatened species, while emphasizing the importance of maintaining habitat heterogeneity.

Keywords: Dietary niche; DNA metabarcoding; Ungulates; Coexistence; Conservation

INTRODUCTION

Understanding the persistence of species diversity remains a core issue in ecological research (Chesson, 2000). As global biodiversity loss intensifies, this issue has gained urgent practical significance (Butchart et al., 2010; Cardinale et al., 2012; Johnson et al., 2017). Foundational ecological theory offers several perspectives on species coexistence. Darwin's principle of divergence suggests that natural selection promotes ecological differentiation, driving species to evolve toward distinct and complementary niches (Darwin, 1859; Pfennig & Pfennig, 2010). At the same time, Hardin's principle of competitive exclusion posits that species competing for identical resources cannot stably coexist (Hardin, 1960). A broad body of theoretical and empirical work has since reinforced the central role of niche partitioning in enabling long-term species coexistence (Levine & HilleRisLambers, 2009; Schoener, 1974). Among the various niche dimensions, dietary segregation is particularly informative for understanding interspecific interactions and competitive dynamics. Recent advances such as DNA metabarcoding have enhanced the resolution of dietary niche analysis in natural communities. For instance, Pansu et al. (2022) and Shao et al. (2021) uncovered dietary differentiation within large herbivore and carnivore assemblages in the African savanna and mountainous regions of southwest China, respectively. Despite such progress, empirical investigations have largely focused on species-rich biomes such as forests and grasslands. In contrast, deserts, as the driest and most resource-limited environments on Earth, have received far less attention. How multiple large herbivores occupying equivalent trophic positions manage to coexist under severe nutritional constraints in such environments remains an intriguing and unresolved question.

Robust delineation of dietary niches requires comprehensive, high-resolution data on foraging composition. Conventional approaches —such as direct observation and microscopic examination of fecal contents—have been widely employed in herbivore diet studies (Matthews et al., 2020;

Received: 16 November 2025; Accepted: 05 December 2025; Online: 16 January 2026

Foundation items: This work was supported by the Project of Management of Endangered Wildlife Populations and Habitats in Kalamaili Nature Reserve (KS-QXD-2024) and the National Key R&D Program of China (2022YFC2601601).

*Corresponding authors, E-mail: ernest8445@163.com; hudf@bjfu.edu.cn

Stewart, 1967; Storr, 1961). However, these approaches are constrained by observer subjectivity and limited taxonomic resolution, often failing to distinguish morphologically similar plant taxa or to quantify relative dietary components. Consequently, such assessments tend to overrepresent conspicuous or morphologically distinctive plant fragments, particularly those resistant to digestion, thereby introducing systematic bias into dietary profiles (Gill et al., 1983; Westoby et al., 1976). Recent advances in high-throughput sequencing have transformed dietary analysis through DNA metabarcoding, particularly via amplification of the chloroplast *trn*L-P6 marker. This technique enables sensitive and precise reconstruction of herbivore diets from fecal material, yielding quantitative insights into plant community use with minimal observer bias (Ando et al., 2020; Valentini et al., 2009). DNA metabarcoding has proven especially effective for characterizing dietary niche structure and interspecific competition in coexisting herbivores (Kartzinel et al., 2015; Pansu et al., 2022), providing a powerful molecular framework for investigating ecological interactions in resource-limited environments.

The Kalamaili Nature Reserve (KNR), located along the eastern margin of the Junggar Gobi, spans approximately 14 700 km^2 and represents one of the largest protected arid ecosystems in China. Globally, it exemplifies a temperate desert biome and serves as a critical refuge for desert-dwelling ungulates (Cao et al., 2025). KNR remains the only region in China where temperate desert ungulates are concentrated at such scale. It encompasses the historic native range of Przewalski's horse (PH; *Equus ferus przewalskii*; IUCN status: Endangered), which became extinct in the wild in 1969 and has since been reintroduced to this site—now the largest global release area for this species. The reserve also supports over 80% of the Asiatic wild ass (AWA; *Equus hemionus*; IUCN status: Near Threatened) population in China, representing the densest and most continuous distribution of this species nationally. In addition, goitered gazelle (GG; *Gazella subgutturosa*; IUCN status: Vulnerable) maintains a population within the reserve that constitutes approximately one-quarter of the global total (Xia et al., 2014; Xu et al., 2022). Both AWAs and GGs are native inhabitants of this desert ecosystem, whereas PHs were reintroduced in 2001. The co-occurrence of these three threatened ungulate species under extreme environmental constraints makes KNR an ideal natural model for investigating competitive interactions and mechanisms of ecological coexistence among sympatric large herbivores in deserts.

To address current knowledge gaps in understanding reintroduction outcomes and niche organization in desert ungulate assemblages, this study applied DNA metabarcoding to assess dietary niche partitioning among PHs, AWAs, and GGs within KNR. The investigation focused on two key questions: 1) What niche structure characterizes reintroduced PHs relative to native species occupying equivalent trophic levels? 2) How is niche partitioning structured among these large herbivores in a severely resource-limited environment? The findings obtained in this study are expected to provide theoretical support for assessing the survival status of endangered species during reintroduction processes and inform conservation strategies for the management of ungulates in desert ecosystems.

MATERIALS AND METHODS

Study area

KNR is situated in the central Eurasian interior, along the eastern edge of the Junggar Basin in northern Xinjiang, China (E88°30′–90°03′ and N44°40′–46°00′). The region experiences a typical temperate continental arid climate characterized by very low annual precipitation (159.1 mm) and high annual evaporation (2 090.4 mm), classifying it as an extreme arid environment (Cao et al., 2025). KNR occupies the transitional zone between the Mongolian subregion and the Kazakhstan-Middle Asia subregion of the Eastern Palearctic biogeographic realm (Dengler et al., 2020). It encompasses a mosaic of desert landscapes, including loess desert (LD), sandy desert (SD), gravel desert (GD), and sandy gravel desert (SGD), and serves as a critical refuge for rare and threatened desert-adapted fauna in the mid-latitude deserts and steppes of Central Asia. KNR supports the highest diversity of wild ungulates among nature reserves in China (Xu et al., 2022). PHs were first reported in the region in 1881. However, anthropogenic pressures, including hunting, overgrazing by livestock, and mineral extraction, led to a gradual population collapse, resulting in local extinction by the 1960s. Reintroduction efforts commenced in 1985 with translocations from zoos in Western countries, and in 2001, a formal wild-release and restoration initiative was launched in KNR (Turghan et al., 2022), resulting in a current free-ranging PH population of 339 individuals. Native AWA and GG have also faced threats from poaching, habitat degradation, and severe climatic events, yet both species have persisted within the region (Li et al., 2019). Since the establishment of KNR, their populations have increased steadily, with current estimates exceeding 3 800 AWAs and 11 400 GGs.

Sample collection

Field sampling was conducted from 2–5 September 2023. Four trained personnel surveyed the reserve using an off-road vehicle, systematically dividing KNR into four geographic regions (east, south, west, and north), each sampled on a separate day via vehicle-based transects. Ungulates were located using binoculars, and observers maintained distance until defecation was observed. Once multiple individuals defecated, fresh fecal samples were collected using sterile 5 mL collection tubes. For each sample, metadata including sample ID, collection time, species identity, habitat type, and GPS coordinates (one location per herd) were recorded. All available fecal boluses or pellets from each defecation event were collected to ensure representative sampling. Morphological features were used to distinguish individuals and minimize the risk of duplicate sampling. Repeated defecation events by the same individual were rare due to the short observation window per herd.

A total of 189 fresh fecal samples were collected. Following sample screening, 174 samples were retained for molecular analysis, comprising 94 from AWAs, 56 from GGs, and 24 from PHs (Figure 1; Supplementary Table S1). Samples were stored on dry ice in the field and during transport and subsequently transferred to Beijing Forestry University (China) for storage at −20°C. DNA extraction was performed on all 174 samples within one week of laboratory arrival.

DNA extraction

Fecal samples were first transferred from the collection tubes into sterile homogenization bags. Each sample was manually

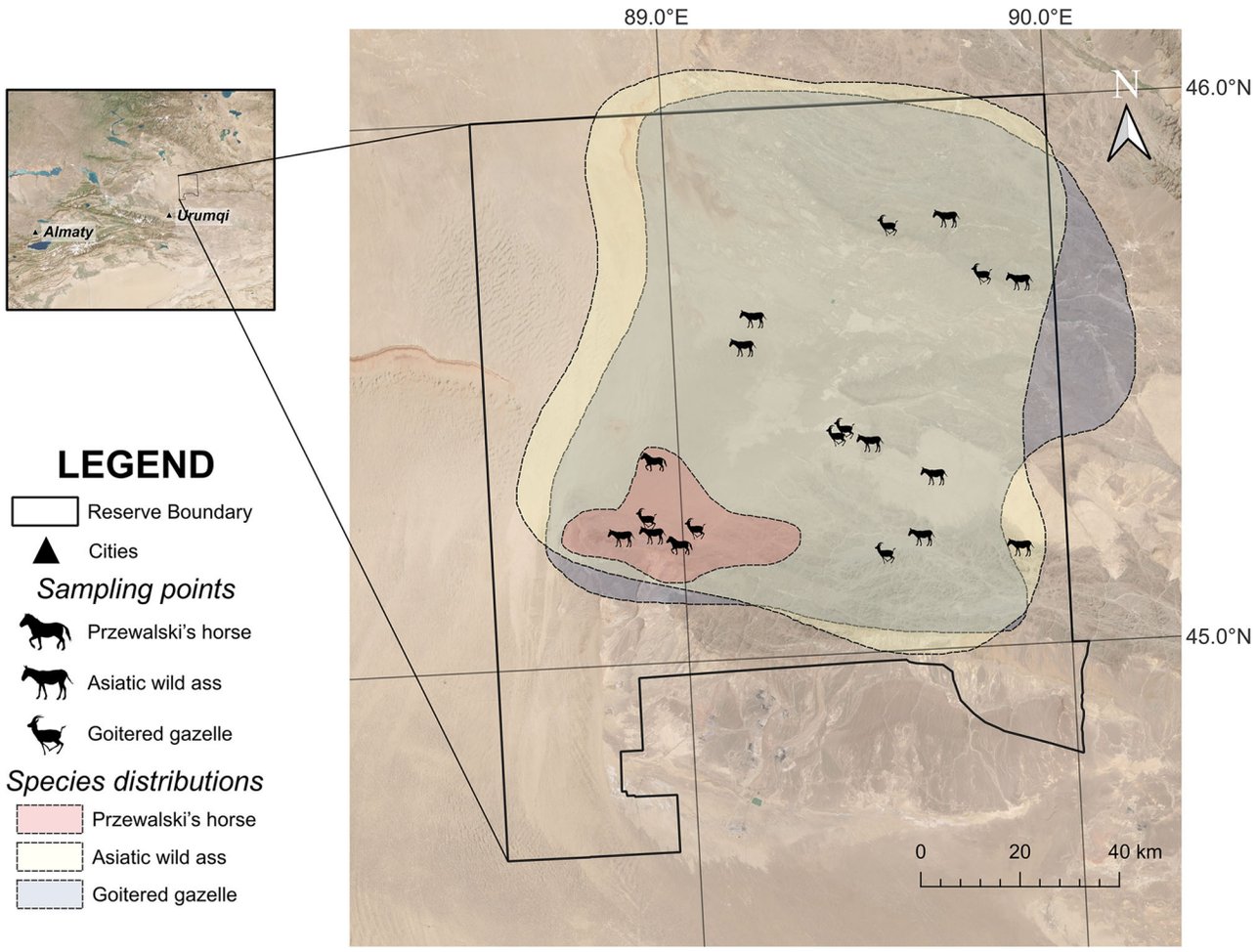

Figure 1 Fecal sampling points in Kalamaili Nature Reserve (KNR)

Black outline indicates KNR boundary. Animal icons represent herd locations from which samples were collected. Colored shaded areas represent main distribution ranges of the three ungulate species within KNR, based on the KNR scientific survey report and field observations.

homogenized by kneading the bag and crushing the fecal material using a pestle applied externally. Approximately 100 mg of the homogenized material was then transferred into 2 mL bead-beating lysis tubes (Disruptor Tubes; Omega Bio-tek, Norcross, GA, USA) using disposable sterile forceps. Each tube received 725 μL of SLX-Mlus Buffer (Omega Bio-tek, Norcross, GA, USA), after which samples were subjected to mechanical disruption at 70 Hz for 5 min using a Tissuelyser® tissue grinder (Shanghai Jingxin Industrial Development, Shanghai, China) to facilitate lysis of plant cell walls. Total genomic DNA was extracted using an E.Z.N.A.® Soil DNA Kit (Omega Bio-tek, Norcross, GA, USA) following the manufacturer's instructions, with a minor modification in the final elution step, wherein ddH_2O was used instead of the supplied elution buffer to facilitate downstream polymerase chain reaction (PCR) amplification. DNA purity was assessed using a NanoDrop 2000 spectrophotometer (Thermo Fisher Scientific, Waltham, MA, USA), DNA concentration was quantified using the Qubit™ 1X dsDNA HS Assay Kit on a Qubit™ 4 Fluorometer (Thermo Fisher Scientific, Waltham, MA, USA), and DNA integrity was evaluated via 1% agarose gel electrophoresis.

Metabarcoding PCR amplification and sequencing

The chloroplast *trn*L (UAA) P6 loop region was amplified using the universal primer pair: Forward (*g*): 5'-GGGCAATCCTGAGCCAA-3' and Reverse (*h*): 5'-CCATTGAGTCTCTGCACCTATC-3', which offer robust performance and broad taxonomic coverage, particularly for degraded DNA from fecal sources (Taberlet et al., 2007). A unique 9-base tag was added to the 5' end of each primer, with identical tag sequences applied to forward and reverse primers within a single PCR reaction. All tags differed by at least four bases, enabling multiplexing across PCR products from each library prior to high-throughput sequencing. PCR was conducted in 20 μL volumes containing 2 μL of fecal DNA extract, 0.5 μL of each primer, 10 μL of 2× Es Taq MasterMix (CoWin Biotech, Taizhou, Jiangsu, China), and 7 μL of ddH_2O. Thermal cycling included an initial denaturation at 95°C for 3 min, followed by 45 cycles at 94°C for 30 s (denaturation), 55°C for 30 s (annealing), and 72°C for 10 s (extension), with no final extension step. Reactions were held at 4°C upon completion. All samples were amplified in triplicate to mitigate stochastic effects. Each PCR batch included at least three negative controls (with ddH_2O only) and three positive controls (DNA extracted from known plant material) to monitor potential contamination. PCR products from replicate reactions of each sample were pooled in equal volumes and purified using VAHTS DNA Clean Beads (Vazyme Biotech, Nanjing, Jiangsu, China) on a 32-well magnetic separation rack (Vazyme Biotech, Nanjing, Jiangsu, China), according to the manufacturer's protocols. Purified amplicon concentrations were measured using the Qubit™ 1X dsDNA HS Assay Kit on a Qubit™ 4 Fluorometer. Equimolar pooling of the purified

amplicons was performed to construct sequencing libraries. Paired-end sequencing (2×150 bp) was carried out on the Illumina NovaSeq 6000 platform (Illumina, San Diego, CA, USA) at GENEWIZ China Headquarters (Suzhou, China).

Bioinformatics and statistical analysis

Processing of dietary metabarcoding data: Dietary sequence data were processed using OBITools v1.2.13 (Boyer et al., 2016). Paired-end reads were first aligned using the *illuminapairedend* command, and those with alignment scores less than 40 were discarded. Unaligned sequences were removed using the *obigrep* command. Sample identities were assigned using *ngsfilter* based on primer tags, allowing no mismatches in tags and up to two mismatches in primer sequences. Identical reads were merged using *obiuniq*, retaining only per-sample read counts and eliminating duplicate sequences. Low-quality reads were filtered out using *obigrep*, excluding sequences containing ambiguous nucleotides, those shorter than 8 bp or greater than 180 bp, and singleton sequences appearing only once in the entire dataset. The *obiclean* command was used to remove PCR/sequencing errors (sequences with a 1-bp difference and an abundance less than 50% of the dominant sequence). Additional filtering was conducted in R v4.4.3 (R Core Team, 2025).

Taxonomic assignment relied on both local and global reference databases. A regional reference set was compiled by integrating the Dataset of Desert Plant Catalogue in Xinjiang (Sun, 2024) with the vascular plant checklist from the KNR Comprehensive Scientific Expedition. This dataset included 45 families, 229 genera, and 554 species. Chloroplast genome or *trn*L gene sequences for these taxa were downloaded from the NCBI database (including 44 families, 198 genera, and 408 species) (Supplementary Table S2), and *in silico* PCR was conducted on the *trn*L-P6 region using *ecoPCR* to generate a curated local database. This reference encompassed 97.8% of families, 86.5% of genera, and 73.6% of species of Xinjiang desert plants, offering comprehensive coverage of dominant plant groups in the study area. A global reference database was also generated by performing *in silico* PCR on all plant nucleotide sequences from the EMBL database (release 143) using *ecoPCR*. Taxonomic assignment of sequences was performed using *ecotag* against both local and global reference databases. Annotated sequences were then converted into a sequence-by-sample matrix using the *obitab* command. To eliminate low-abundance false positives caused by tag-jumping during amplicon sequencing, reads representing less than 1% of total reads in each sample were removed. Sequences with identity scores below 80% were also discarded to eliminate potential chimeras and highly degraded sequences (Pansu et al., 2022). Samples with fewer than 100 000 total reads were excluded to ensure high coverage in dietary identification.

Retained sequences were defined as molecular operational taxonomic units (mOTUs) for downstream analysis. Taxonomic assignments of mOTUs prioritized local database matches (marked as “Local”), unless the global reference provided a more specific identification with higher sequence identity, in which case the global assignment was adopted (marked as “Global”). For unresolved taxonomic ranks, standardized naming conventions were applied: if genus-level assignment was not possible, the genus was labeled as scientific_name gen. indet., and the species as scientific_name gen. et sp. indet.; if only the genus was resolved, the species was labeled as scientific_name sp. Taxonomic nomenclature was cross-validated using the Angiosperm Phylogeny Group IV (APG IV) system via the iPlant database (https://www.iplant.cn/). Relative read abundance (RRA) was calculated for each mOTU across samples using the *sweep* function in R. RRA was selected as the primary metric for downstream analyses based on several factors: 1) Studies in large herbivores have demonstrated a strong correlation between trnL-P6-based RRA and actual intake, as validated through feeding trials and stable isotope data (Craine et al., 2015; Kartzinel et al., 2015; Willerslev et al., 2014); 2) Compared to frequency of occurrence (FOO), RRA more accurately reflects feeding proportions, making it better suited for assessing dietary preferences in large herbivores (Zhu et al., 2023); and 3) RRA-based evaluations of resource partitioning yield results qualitatively consistent with presence-absence methods across diverse taxa, including large herbivores (Hemprich-Bennett et al., 2021; Pansu et al., 2019; Pringle et al., 2019).

Food web structure, niche width, and overlap: Bipartite food webs were constructed at both the family and genus levels to illustrate trophic interactions between ungulates and their dietary plant taxa, using the *plotweb* function from the *bipartite* package in R (Dormann et al., 2008). Only genera with RRA values exceeding 0.1% were retained for analysis. Levins’ niche width for each sample was calculated based on the RRA matrix of mOTUs using the *niche.width* function in *spaa* (Zhang, 2025). Pairwise dietary niche overlap between species was estimated using Pianka’s index via the *niche.overlap.pair* function in *spaa*. Boxplots depicting niche width and niche overlap were generated using *ggplot2* (Wickham, 2016), and statistical comparisons between groups were assessed using Wilcoxon rank-sum tests implemented through the *ggpubr* package.

Interspecific dietary dissimilarity: Bray-Curtis dissimilarities among samples were calculated using the *vegdist* function in the *vegan* package (Oksanen et al., 2007). Non-metric multidimensional scaling (NMDS) was performed on the resulting dissimilarity matrix using the *metaMDS* function, incorporating species identity as the grouping variable. Stress values were used to assess dimensional fit. Permutational multivariate analysis of variance (PERMANOVA) was performed using the *adonis2* function with 999 permutations to determine group-level differences, reporting R^2 and associated *P* values. NMDS plots were visualized using *ggplot2*.

Correlation between geographic distance and dietary variation: Pairwise geographic distances between samples were calculated using the *distm* function in the *geosphere* package (Hijmans et al., 2024) in R. To evaluate spatial structuring of dietary profiles, Mantel tests were conducted using the *mantel* function in the *vegan* package, correlating the Bray-Curtis dissimilarity matrix (based on RRA) with the geographic distance matrix. Spearman rank correlation coefficients were calculated with 9 999 permutations, yielding Mantel statistic R and associated *P* values. Results were visualized with scatter plots generated in *ggplot2*, including linear regression lines with 95% confidence intervals.

Dietary niche variation across desert types: To evaluate habitat-specific dietary patterns, samples were grouped according to four major desert types in the KNR: LD, SD, GD, and SGD. Following the approach used for species-based

analyses, dietary dissimilarity was assessed via NMDS using the *metaMDS* function, with habitat grouping incorporated into PERMANOVA using the *adonis2* function, both from the *vegan* package. Dietary niche width and niche overlap were also calculated for each desert type using the *niche.width* and *niche.overlap.pair* functions in *spaa*, followed by visualization using *ggplot2*. Due to the restricted distribution of reintroduced PHs, which were primarily concentrated near the *Qiaomuxibai* release site, this species was excluded from habitat-based comparisons. Only the two native species (AWA and GG) were included. In addition, as GGs were rarely observed in SD and no samples were obtained from this habitat, SD was excluded from the final analysis.

RESULTS

Dietary composition of threatened ungulates

Metabarcoding sequencing generated a total of 117 470 027 raw reads. Subsequent to dereplication, 1 375 646 unique reads were obtained, with 108 882 clean reads retained after quality control. Taxonomic annotation and the removal of low-abundance and low-similarity sequences resulted in 77 high-confidence annotated reads. Following the exclusion of samples with insufficient sequencing depth, 162 fecal samples were retained for downstream analysis, including 88 from AWAs, 21 from PHs, and 53 from GGs. These samples ultimately yielded 64 distinct plant mOTUs. Among these, 35 (54.7%) were identified to species, 53 (82.8%) to genus, and all 64 (100%) to family level (Supplementary Table S3). After merging mOTU taxonomic assignments with their corresponding RRA, a total of 38 dietary plant taxa from 14 families were identified, including 31 (81.6%) assigned to genus and 27 (71.1%) to species level (Supplementary Table S4). Asteraceae showed the highest RRA (39.43%), while Amaranthaceae represented the most taxonomically diverse family, comprising 12 dietary taxa (Figure 2; Supplementary Table S4).

Although AWAs and GGs occupied more similar geographic ranges, AWAs shared greater dietary similarity with PHs. At the family level, both AWAs and PHs primarily consumed Asteraceae (31.81%; 43.98%), Tamaricaceae (25.30%; 17.18%), Amaranthaceae (21.68%; 28.10%), and Poaceae (10.76%; 4.87%), which together accounted for nearly 90% of the AWA diet and over 94% of the PH diet. In contrast, GGs consumed a narrower range of plant taxa, with high relative abundances in Asteraceae (50.27%) and Tamaricaceae (45.72%), which collectively comprised more than 95% of total dietary intake (Figure 2; Supplementary Table S4).

At the genus level, Artemisiinae gen. indet. (31.55% for AWA; 43.84% for PH), *Reaumuria* (25.14%; 17.17%), and *Kraschenninnikovia* (15.66%; 25.12%) were the dominant dietary components for both AWAs and PHs. Additional dietary taxa consumed by AWAs (RRA>1%) included *Stipa* (6.37%), Hordeinae gen. indet. (2.90%), *Ceratocarpus* (2.83%), *Ephedra* (2.43%), *Atraphaxis* (2.10%), Brassicaceae gen. indet. (2.00%), *Atriplex* (1.78%), *Convolvulus* (1.33%), and *Phragmites* (1.23%). For PHs, other major dietary taxa (RRA>1%) included Hordeinae gen. indet. (2.42%), *Astragalus* (1.93%), *Stipa* (1.64%), *Atraphaxis* (1.26%), *Atriplex* (1.21%), and Brassicaceae gen. indet. (1.12%). In contrast, the diet of GGs was highly specialized, dominated by *Artemisiinae* (50.25%) and *Reaumuria* (45.70%), with all other taxa contributing less than 1% RRA, except for *Pyankovia* (1.98%) (Figure 2; Supplementary Table S4).

Dietary niche width and overlap

To assess interspecific variation in dietary niche structure, statistical analyses were conducted using mOTU-level RRA data (Supplementary Table S5). Levins' niche width and Pianka's niche overlap indices were calculated and compared across species (Figure 3). Both equid species exhibited relatively broad and variable niche widths. The median niche width for AWAs was 4.19 (interquartile range (IQR) 3.31–5.85), while that for PHs was 4.20 (IQR 2.81–4.60), with no statistically significant difference between the two (W=1 130; P>0.05). In contrast, GGs exhibited significantly narrower and more constrained dietary niches, with a median value of 1.23 (IQR 1.11–1.86), significantly lower than those of both AWAs (W=4 554; P<0.000 1) and PHs (W=1 109; P<0.000 1) (Figure 3A).

Regarding dietary niche overlap, the highest overlap was observed between AWAs and PHs (median 0.81, IQR 0.67–0.91), followed by PHs and GGs (median 0.78, IQR 0.45–0.92), with the lowest overlap between AWAs and GGs (median 0.68, IQR 0.49–0.85) (Figure 3B). All pairwise comparisons showed highly significant differences (P< 0.000 1), including the comparisons involving AWA-GG and PH-GG pairs, despite the close phylogenetic relationship and similar physiological structures of AWA and PH.

Interspecific dietary dissimilarity

By projecting interspecific dietary dissimilarity into a low-dimensional space, the spatial distribution of diets among the three sympatric ungulate species can be intuitively visualized. Based on the RRA data of dietary mOTUs, we calculated a Bray-Curtis dissimilarity matrix among individuals (Supplementary Table S6) and performed an NMDS analysis. PERMANOVA was then conducted to test for non-parametric statistical differences in dietary dissimilarity among species groups (Figure 4). The NMDS stress value was 0.12, indicating a good fit between the reduced-dimensional ordination and the actual ecological distances. The overall comparison of the three sympatric ungulates (Figure 4A) showed that although species grouping explained a relatively small portion of inter-individual dietary variation (R^2=0.04), the dietary dissimilarity among species remained highly significant (P=0.007). This result indicates that inter-individual dietary differences were significantly influenced by species identity rather than random variation.

Pairwise comparisons revealed that the strongest interspecific separation occurred between PH and GG, with species grouping accounting for 25% of dietary variance (R^2=0.25; P=0.001) (Figure 4B). Significant dietary divergence was also detected between the two equid species (R^2=0.08; P=0.001), despite the substantial overlap in their dietary space and near-nested distribution of PHs within the broader dietary profile of AWAs (Figure 4C). In contrast, although AWAs and GGs showed minimal niche overlap in previous analyses, species identity explained only 1% of their dietary variance and was not statistically significant (R^2=0.01; P=0.179) (Figure 4D). Despite this low explanatory power, these two species formed distinct dietary clusters, indicating that species grouping alone is insufficient to explain the dietary variation observed and that other ecological or environmental factors may be involved. From the perspective of dietary space distribution, individual dietary points of AWAs and GGs were more dispersed. In contrast, those of PHs were more

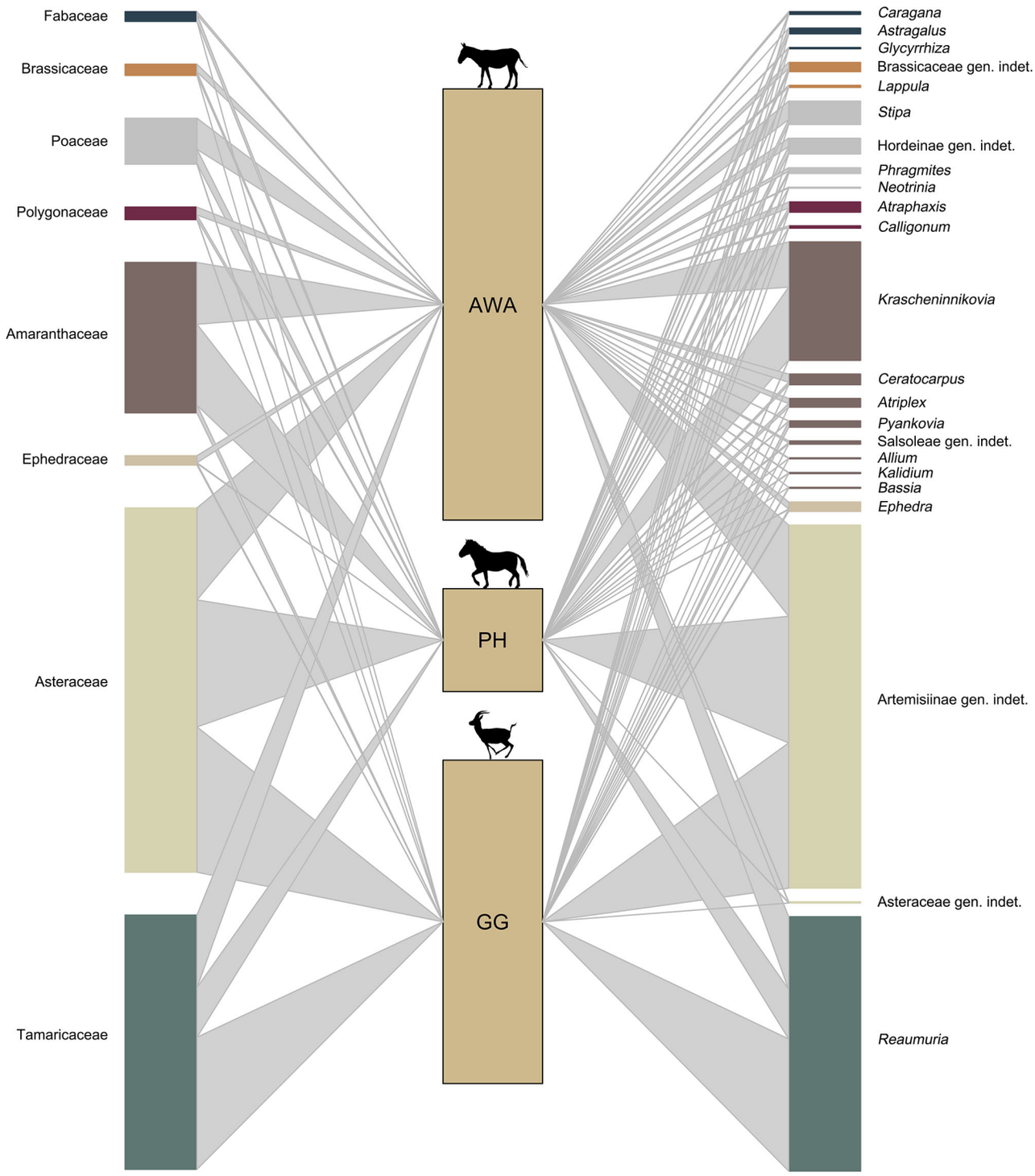

Figure 2 Dietary composition of the ungulates

Central boxes represent the three focal ungulate species, ordered from top to bottom as AWA, PH, and GG. Box size reflects relative number of individuals sampled per species. Left-side boxes represent plant families, and right-side boxes represent plant genera; box size represents relative read abundance (RRA) for each plant taxon. Line width connecting species to plant taxa indicates relative feeding abundance. Box colors correspond to plant families.

concentrated (i.e., exhibiting lower intraspecific variation). Therefore, the relatively high intraspecific variation in both AWAs and GGs may have diluted the interspecific differences.

Geographic distance and intraspecific dietary dissimilarity

To investigate spatial drivers of intraspecific dietary variation in AWAs and GGs, Mantel tests were conducted to assess correlations between geographic distance matrices (Supplementary Tables S7–S8) and Bray-Curtis dietary dissimilarity matrices of dietary composition for each species. Spearman's rank correlation coefficients revealed strong positive correlations between geographic distance and dietary dissimilarity in both species (Figure 5). In AWAs, dietary dissimilarity exhibited a moderate increase with increasing geographic distance (R=0.2653, *P*=0.0001; Figure 5A). For GGs, although individuals within the same locality (i.e.,

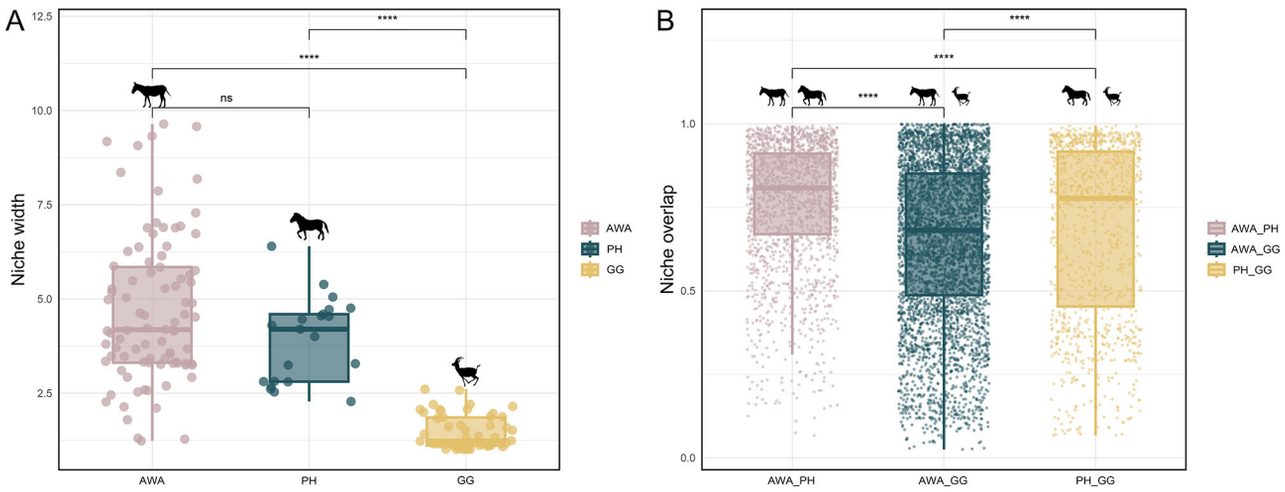

Figure 3 Dietary niche width and overlap of the ungulates

A: Individual dietary niche width of the three ungulate species, presented left to right as AWA, PH, and GG. Each point represents niche width of an individual animal. B: Pairwise dietary niche overlap of the three ungulate species, presented left to right as AWA vs. PH, AWA vs. GG, and PH vs. GG. Each point represents overlap between a pair of individuals from the two species. ns: Not significant; ****P<0.0001.

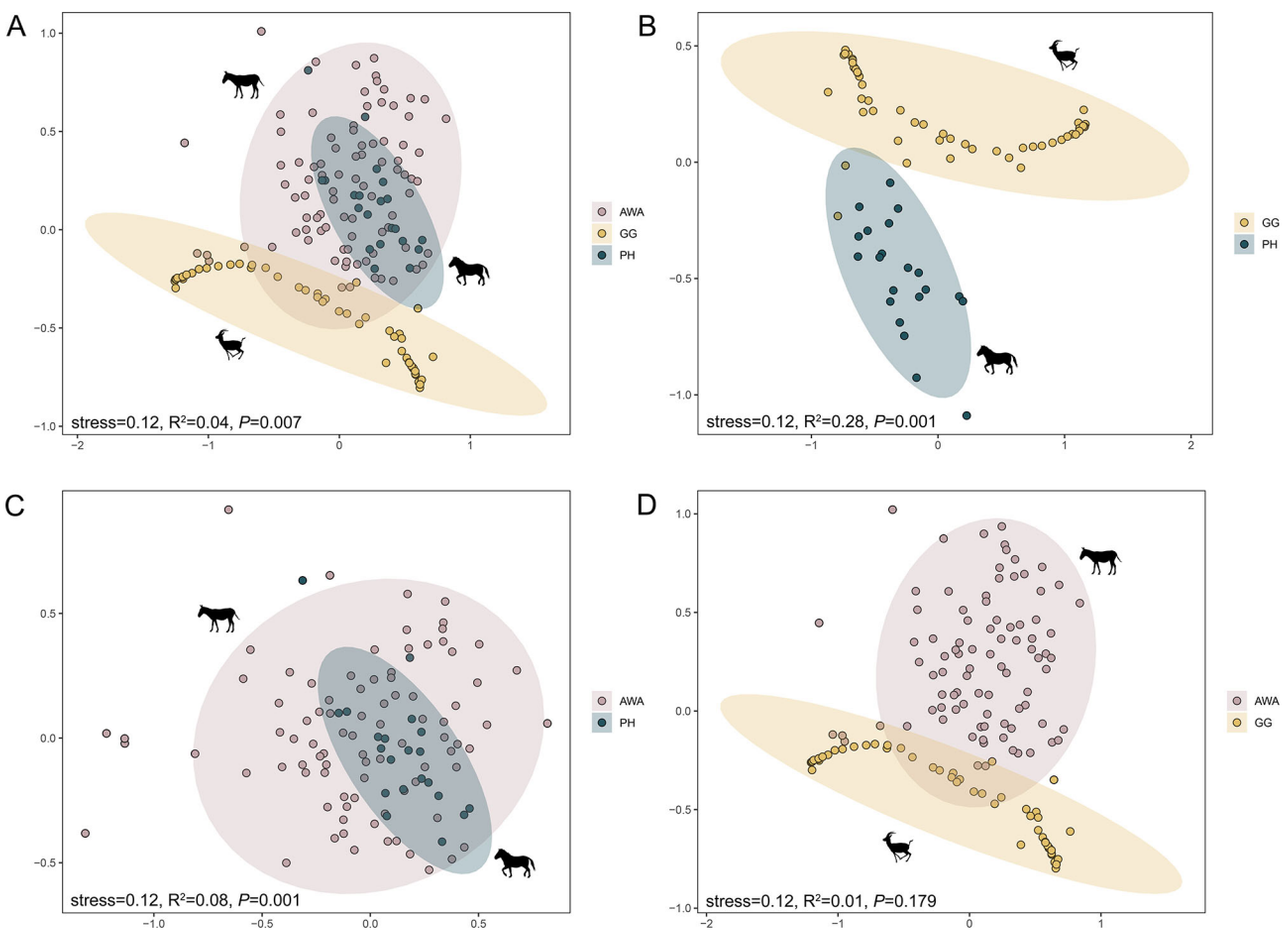

Figure 4 NMDS of dietary dissimilarity among species

A: Dietary dissimilarity among the three ungulate species. B: Dietary dissimilarity between PH and GG. C: Dietary dissimilarity between AWA and PH. D: Dietary dissimilarity between AWA and GG. Each point represents projection of dietary dissimilarity between individuals in two-dimensional space. Closer distances between points indicate greater dietary similarity between individuals, and vice versa. NMDS stress values and PERMANOVA test results are shown in the lower left of each panel.

geographic distance=0) showed relatively low dietary dissimilarity (mean=0.29, compared to 0.37 for AWAs), dietary dissimilarity varied substantially with increasing geographic distance (R=0.4064, P=0.0001; Figure 5B). Linear regression indicated that every 10 km of geographic distance between individuals corresponded to an average increase in dietary dissimilarity of 0.014 for AWAs and 0.046 for GGs, over a three-fold difference. These results suggest that spatial heterogeneity in habitat conditions influence dietary composition in both species, with GGs exhibiting a markedly

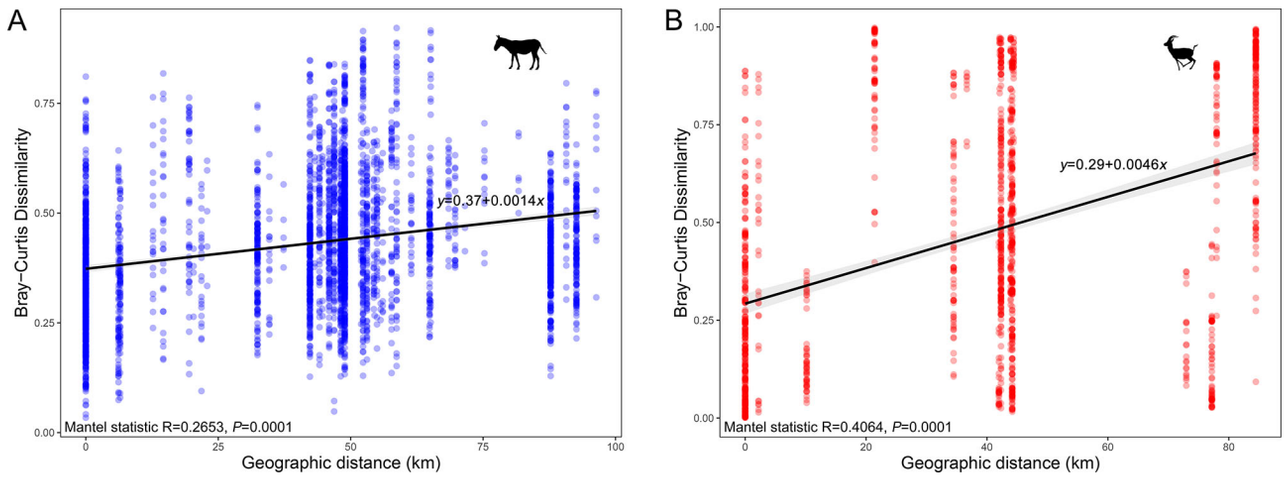

Figure 5 Correlation between geographic distance and dietary dissimilarity

A: Correlation for AWA. B: Correlation for GG. Each point represents a pairwise comparison between two individuals, plotting geographic distance against corresponding dietary dissimilarity. Mantel test results are shown in the lower left of each panel, and linear regression results are displayed above the regression lines.

greater sensitivity to geographic variation in food resource use.

Patch-level heterogeneity in dietary niche partitioning

The KNR, where AWAs and GGs coexist, comprises four major desert habitat types: LD, SD, GD, and SGD (Figure 6; Supplementary Figure S1). Each desert type spans a substantial spatial area, making cross-habitat movement by individuals within a single foraging-to-defecation interval unlikely. Based on this spatial structure, NMDS of dietary dissimilarity, along with niche width and overlap analyses, was performed separately for each desert type to assess fine-scale habitat-driven dietary variation in both species (Figure 7). NMDS combined with PERMANOVA revealed that dietary composition differed significantly across desert types in both AWAs (R^2=0.2, P=0.001) and GGs (R^2=0.29, P=0.002), indicating that habitat type strongly influenced dietary composition in these sympatric ungulates (Figure 7A, B). Further analysis of dietary niche width revealed opposing trends between the species across the three habitats (SD excluded due to lack of GG samples), suggesting divergent resource use strategies. Among AWAs, dietary niche width was highest in GD (median 5.48), followed by SGD (median 5.03), and lowest in LD (median 4.48). In contrast, GGs exhibited the highest dietary niche width in LD (median 1.88), followed by SGD (median 1.16), and lowest in GD (median 1.15). Thus, the habitat in which AWAs demonstrated the broadest dietary niche width was where GGs showed the narrowest, and vice versa, suggesting spatial niche complementarity. SGD represented an intermediate patch for both species. Dietary niche overlap analysis further supported this pattern. The highest interspecific niche overlap —and therefore the greatest potential for competitive interaction—was observed in SGD (median 0.85, IQR 0.69 to 0.95), compared to LD (median 0.72, IQR 0.59 to 0.89) and GD (median 0.52, IQR 0.33 to 0.69) (Figure 7E). This phenomenon of niche complementarity indicates that the widely sympatric AWAs and GGs in the KNR exhibit distinct resource partitioning across different habitat patches and cryptic niche partitioning.

DISCUSSION

Using fecal DNA metabarcoding targeting the chloroplast *trn*L-P6 region, this study elucidated patterns of dietary niche partitioning among three threatened ungulate species inhabiting the arid deserts of northwestern China. High-resolution dietary profiles were obtained for all species, enabling detailed interspecific comparisons. Artemisiinae emerged as the most intensively consumed plant group across all three species, reflecting its ecological dominance within the local flora (Xu et al., 2016) and potential functional role as a valuable moisture source in this arid environment (Van Driessche et al., 2025). Amaranthaceae, representing the most taxonomically diverse family within the reserve, contributed the highest richness of dietary plant taxa, underscoring its importance in sustaining herbivore diversity. In addition to Artemisiinae, other xerophytic shrubs, such as *Reaumuria songarica* and *Krascheninnikovia ceratoides*, ranked prominently among the preferred forage species for both AWAs and PHs. However, GGs displayed a markedly narrower diet, strongly preferring *R. songarica* while largely avoiding *K. ceratoides,* despite its broad availability within the reserve (Xu et al., 2016). Moreover, the equids exhibited greater diversity in the major consumed plant taxa (RRA>1%) relative to GGs, highlighting greater foraging breadth. These findings collectively point to a higher degree of selectivity in GGs and suggest trophic separation through differential exploitation of dominant plant taxa. The exclusion of *K. ceratoides* from GG diets, despite its widespread presence, and its concurrent importance to both equid species provides strong evidence for resource partitioning between GGs and the two equids within this desert ungulate assemblage.

Niche width quantifies the extent of ecological flexibility and resource exploitation across environmental gradients. Among the three desert ungulates examined, AWAs and PHs displayed substantial variation in dietary niche width, whereas GGs maintained consistently narrow diets with minimal individual variation. This disparity reinforces the classification of the sympatric equid species as dietary generalists, exhibiting greater foraging plasticity in response to spatial and temporal fluctuations in plant availability. In contrast, GGs function as dietary specialists, restricting intake to a narrow subset of plant species regardless of environmental heterogeneity (Shipley et al., 2009). These divergent foraging strategies align with the optimal foraging theory, which predicts generalist behavior in “searchers” and specialization

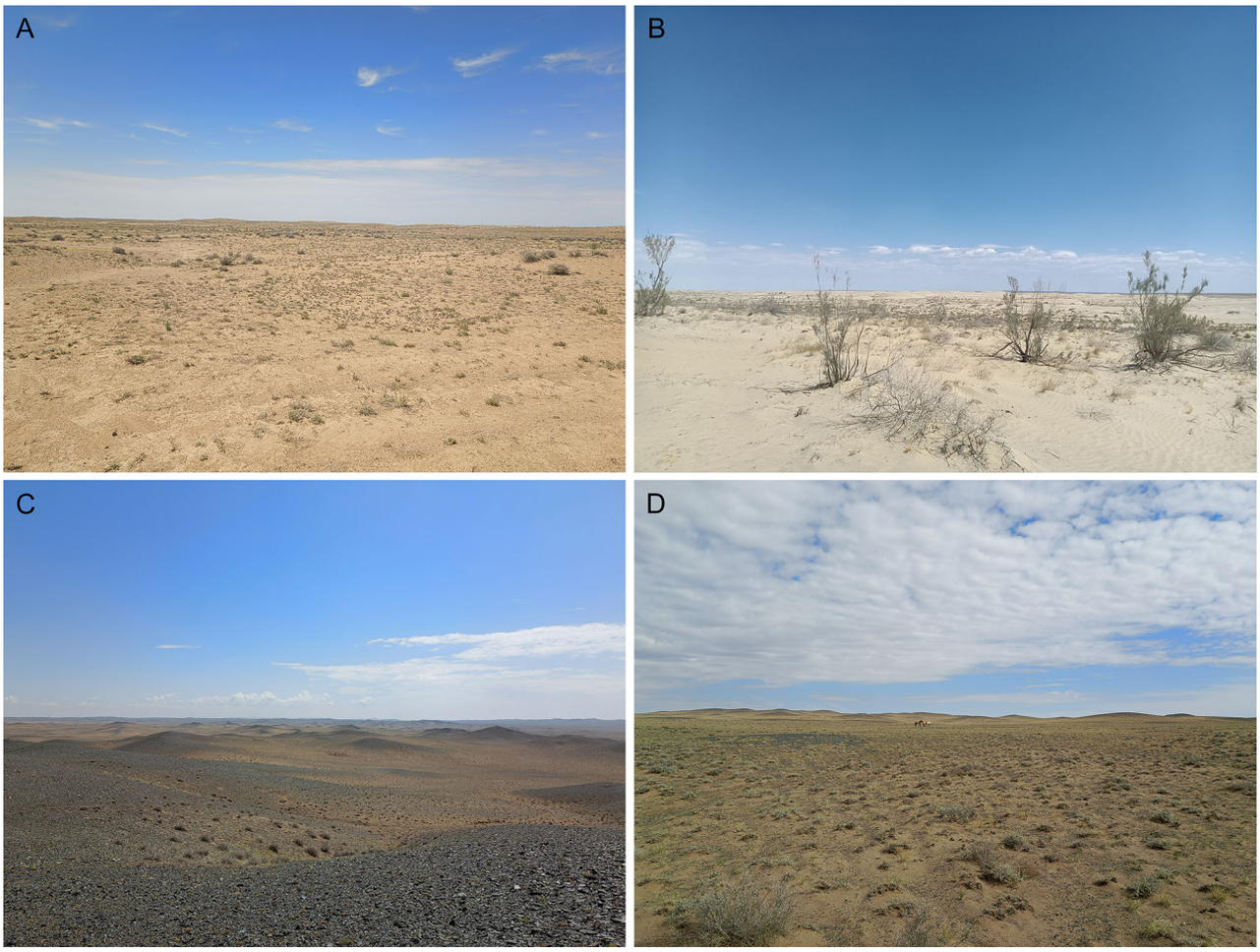

Figure 6 Representative desert habitat types within Kalamaili Nature Reserve (KNR)

A: Loess desert (LD), primarily found in the central reserve and north of the Kalamaili Mountains at elevations of 800–1 300 m above sea level (a.s.l.), characterized by dry, compact yellow soil. B: Sandy desert (SD), located in the western, southern, and southwestern regions of the reserve at elevations of 500–900 m a.s.l., representing an extension of the Gurbantünggüt Desert with predominantly fixed and semi-fixed sand ridges and dunes. C: Gravel desert (GD), located in the northwestern and northern regions of the reserve at elevations of 900–1 300 m a.s.l., defined by a gravel-covered surface commonly referred to as the “Black Gobi”. D: Sandy gravel desert (Gobi; SGD), distributed across the southern and southeastern regions of the reserve, including the main parts of the Kalamaili mountainous hills at elevations of 500–1 400 m a.s.l., where the surface consists of mixed sand and gravel. Photos by An-Qi Wang (A–B) and Zhi-Chao Zhou (C–D).

in “handlers” (Charnov, 1976; MacArthur & Pianka, 1966). “Searchers” allocate more time to locating food and less to processing it, whereas “handlers” emphasize processing efficiency over search effort. As hindgut fermenters, AWAs and PHs possess short digesta retention time and low digestive efficiency, favoring a high-throughput, low-yield foraging strategy that necessitates broad dietary inclusion to meet energetic demands (Clauss et al., 2023). In contrast, GGs are ruminants that require prolonged rumination and selective intake of nutrient-dense forage, consistent with a handler strategy (Hanley, 1982). Similar patterns are evident in African savanna herbivores, where smaller-bodied species with higher mass-specific metabolic rates tend to adopt highly selective feeding strategies, whereas larger-bodied species prioritize forage volume over quality due to energetic scaling constraints (Pansu et al., 2019).

Dietary niche overlap provides a critical metric for evaluating interspecific competition within ecological communities (du Preez et al., 2017; Vogel et al., 2019). In this study, dietary niche overlap between AWAs and GGs was markedly lower than that observed between the two equids or between PHs and GGs, implying reduced dietary competition between the two native species. As native inhabitants of the northwestern desert, AWAs and GGs appear to have achieved stable coexistence through long-term natural competition. In contrast, PHs exhibited substantial dietary niche overlap with both native taxa, reflecting an absence of distinct trophic separation despite over 20 years of rewilding efforts (Xia et al., 2014). This pronounced niche convergence highlights the potential for competitive interactions with native ungulates and underscores the need for continued monitoring of the nutritional ecology of PHs to ensure the long-term success of reintroduction programs and minimize disruption to existing community structure.

The distribution of dietary niches of sympatric ungulates in two-dimensional space was significantly influenced by species identity, indicating that species grouping can partially explain dietary variation among ungulates, rather than being solely the result of random variation or other external factors. However, in pairwise comparisons between AWAs and GGs, species grouping alone failed to account for the observed variation, suggesting a stronger influence of other ecological or spatial drivers. PHs exhibited markedly lower intraspecific dietary variation compared to the two native species, consistent with

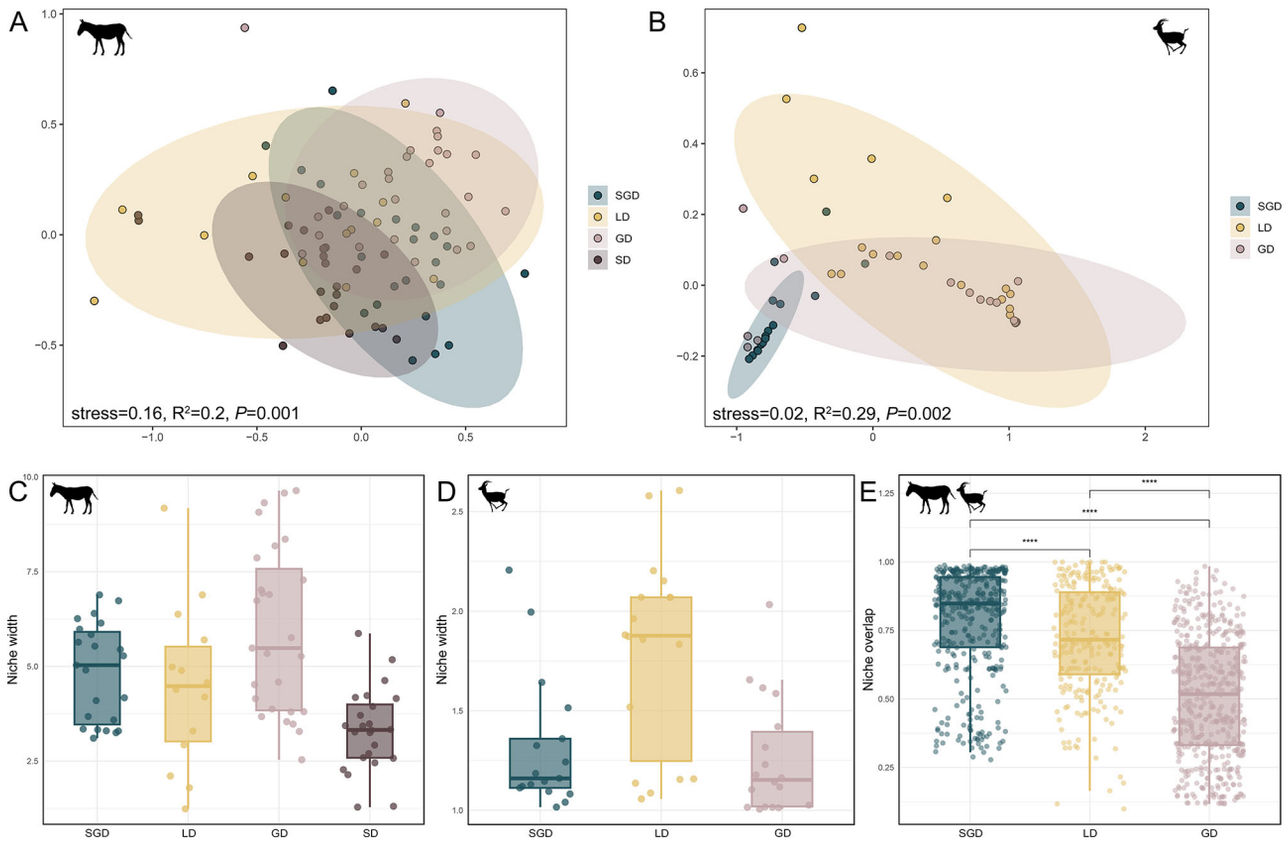

Figure 7 Dietary niche partitioning among different desert types

A–B: NMDS of dietary dissimilarity between different desert types for AWA (A) and GG (B). C–D: Dietary niche width for AWA (C) and GG (D) across different desert types. E: Dietary niche overlap between AWA and GG across desert types. NMDS stress values and PERMANOVA test results are shown in the lower left of panels A and B. ****P<0.0001.

their restricted geographic range, primarily localized around the *Qiaomuxibai* release site (Cao et al., 2025). In contrast, AWAs and GGs occupied broader geographic ranges across the reserve and exhibited greater dietary divergence among individuals. Notably, dietary data from GGs arranged in an approximately linear configuration in two-dimensional space, suggesting that spatial heterogeneity may be a dominant factor driving dietary differentiation within this species. Mantel tests revealed significant positive correlations between geographic distance and dietary dissimilarity in both AWAs and GGs, with GGs showing a steeper slope of increase. This trend likely reflects the contrast between the selective foraging strategy of GGs and the opportunistic behavior observed in AWAs. High dietary selectivity increases the sensitivity of GGs to local variation in plant availability, thereby amplifying spatial dietary divergence. Such selective resource use may also reduce interspecific competition by minimizing dietary overlap with AWAs (Lopes et al., 2015; Milinski, 1982). These findings highlight the need for fine-scale, site-specific resource management to support effective conservation of GGs.

Pronounced dietary dissimilarity between AWAs and GGs across desert habitat types provides strong evidence for patch-level heterogeneity in resource use by these two native species. Habitat-specific availability exerts a strong influence on dietary niche width, with reduced resource availability generally promoting niche expansion to maintain adequate intake (MacArthur & Levins, 1967; MacArthur & Pianka, 1966; Perry & Pianka, 1997). Within shared habitat patches, AWAs and GGs exhibited contrasting dietary niche widths, indicating complementary use of food resources across spatially distinct environments. This pattern is consistent with the principle of competitive exclusion, which predicts that two species occupying identical ecological niches cannot persist in stable coexistence and instead undergo niche differentiation across dimensions such as habitat use, diet composition, or temporal activity (Hardin, 1960). Evidence from African large-herbivore assemblages similarly demonstrates that interspecific competition drives pronounced ecological niche differentiation, even among functionally similar grazers (grass eaters) and browsers (non-grass eaters) (Pansu et al., 2022). Long-term coexistence and competition between AWAs and GGs in the northwestern deserts of China have likely driven local adaptation, resulting in differential specialization to specific habitat patches and effective resource partitioning that supports stable coexistence (Schoener, 1974). Notably, the greatest dietary niche overlap occurred in habitat patches characterized by intermediate niche width, indicating zones where niche differentiation remains incomplete and competitive pressure is highest. Comparable patterns of dietary niche complementarity facilitating interspecific coexistence have been documented in carnivore assemblages (Shao et al., 2021). These findings highlight intermediate habitat patches as critical targets for biodiversity conservation management, where focused intervention may be necessary to mitigate competitive stress and sustain biodiversity.

This study delineated the dietary profiles of three threatened desert ungulates, providing critical insights for the protection of forage plant communities within the reserve. The results provide an empirical foundation for refining captive management and implementing targeted nutritional

interventions. Particular consideration is warranted for GGs, which exhibited high dietary specialization and may require habitat-specific management to accommodate narrow feeding preferences. The findings also highlighted the need for continued dietary surveillance of reintroduced PHs. In regions where they coexist with native species, supplemental feeding may be necessary during resource-limited periods caused by extreme climatic events, until a distinct and stable nutritional niche is established. Furthermore, this study demonstrated that KNR can provide a viable ecological space for the coexistence of AWAs and GGs. However, the preservation of heterogeneous habitat types within the reserve remains essential to sustaining the niche segregation that underpins their long-term stability.

CONCLUSION

This study employed fecal DNA metabarcoding targeting the chloroplast *trn*L-P6 marker to resolve dietary niche partitioning among three sympatric threatened ungulates inhabiting the northwestern deserts of China. High-resolution quantitative dietary data revealed clear divergence in foraging strategies, with AWAs and PHs characterized as dietary generalists, while GGs exhibited pronounced dietary specialization. Minimal niche overlap was observed between AWAs and GGs, suggesting stable coexistence achieved through long-term natural competition and resource differentiation. In contrast, reintroduced PHs showed substantial dietary overlap with native ungulates, underscoring the importance of continued nutritional monitoring of this species during ongoing establishment in the desert ecosystem. Dietary dissimilarity increased with geographic distance in both native species, with a stronger spatial signal in GGs, highlighting sensitivity to localized resource conditions and the need for spatially targeted conservation measures. Complementary resource use across heterogeneous habitat patches reflected local adaptation and effective resource partitioning, supporting long-term stable coexistence. Notably, the highest competitive intensity occurred within habitat patches characterized by intermediate niche width, identifying these transitional zones as priorities for biodiversity conservation. Collectively, these findings provide a robust ecological framework for guiding the conservation and management of threatened desert ungulates.

DATA AVAILABILITY

The raw sequencing data generated in this study have been deposited in the Science Data Bank (https://doi.org/10.57760/sciencedb.zrdc.00040) and NCBI Sequence Read Archive (SRA) (accession number PRJNA1270768).

SUPPLEMENTARY DATA

Supplementary data to this article can be found online.

SCIENTIFIC FIELD SURVEY PERMISSION INFORMATION

The field survey and sample collection were approved by the Kalamaili Nature Reserve and the Ethics and Animal Welfare Committee of Beijing Forestry University (EAWC_BJFU_2021012).

COMPETING INTERESTS

The authors declare that they have no competing interests.

AUTHOR CONTRIBUTIONS

D.Z. and D.F.H. conceptualized and designed the research. Z.C.Z., L.N.Y., and C.L.S. performed the sample collection. Z.C.Z. and J.S. conducted the laboratory experiments. Z.C.Z. and D.F.C. analyzed the data. Z.C.Z., D.Z., and D.F.H. wrote and revised the manuscript. All authors read and approved the final version of the manuscript.

ACKNOWLEDGMENTS

We acknowledge the staff of Kalamaili Nature Reserve for granting permission and providing support for sample collection. We are also grateful to all colleagues who participated in field sampling. We thank An-Qi Wang for providing photographs of representative habitats in the reserve.

REFERENCES

Ando H, Mukai H, Komura T, et al. 2020. Methodological trends and perspectives of animal dietary studies by noninvasive fecal DNA metabarcoding. *Environmental DNA*, **2**(4): 391–406.

Boyer F, Mercier C, Bonin A, et al. 2016. OBITOOLS: a UNIX-inspired software package for DNA metabarcoding. *Molecular Ecology Resources*, **16**(1): 176–182.

Butchart SHM, Walpole M, Collen B, et al. 2010. Global biodiversity: indicators of recent declines. *Science*, **328**(5982): 1164–1168.

Cao QL, Zhang YJ, Songer M, et al. 2025. Coexistence between Przewalski's horse and Asiatic wild ass in the desert: the importance of people. *Journal of Applied Ecology*, **62**(5): 1078–1090.

Cardinale BJ, Duffy JE, Gonzalez A, et al. 2012. Biodiversity loss and its impact on humanity. *Nature*, **486**(7401): 59–67.

Charnov EL. 1976. Optimal foraging, the marginal value theorem. *Theoretical Population Biology*, **9**(2): 129–136.

Chesson P. 2000. Mechanisms of maintenance of species diversity. *Annual Review of Ecology, Evolution, and Systematics*, **31**: 343–366.

Clauss M, Codron D, Hummel J. 2023. Equid nutritional physiology and behavior: an evolutionary perspective. *Journal of Equine Veterinary Science*, **124**: 104265.

Craine JM, Towne EG, Miller M, et al. 2015. Climatic warming and the future of bison as grazers. *Scientific Reports*, **5**(1): 16738.

Darwin CR. 1859. On the Origin of Species by Means of Natural Selection, or the Preservation of Favoured Races in the Struggle for Life. London: John Murray.

Dengler J, Biurrun I, Boch S, et al. 2020. Grasslands of the palaearctic biogeographic realm: introduction and synthesis. *In*: Goldstein MI, DellaSala DA. Encyclopedia of the World's Biomes. Amsterdam: Elsevier, 617–637.

Dormann CF, Gruber B, Fruend J. 2008. Introducing the bipartite package: analysing ecological networks. *R News*, **8**(2): 8–11.

du Preez B, Purdon J, Trethowan P, et al. 2017. Dietary niche differentiation facilitates coexistence of two large carnivores. *Journal of Zoology*, **302**(3): 149–156.

Gill RB, Carpenter LH, Bartmann RM, et al. 1983. Fecal analysis to estimate mule deer diets. *The Journal of Wildlife Management*, **47**(4): 902–915.

Hanley TA. 1982. The nutritional basis for food selection by ungulates. *Journal of Range Management*, **35**(2): 146–151.

Hardin G. 1960. The competitive exclusion principle. *Science*, **131**(3409): 1292–1297.

Hemprich-Bennett DR, Oliveira HFM, Le Comber SC, et al. 2021. Assessing the impact of taxon resolution on network structure. *Ecology*, **102**(3): e03256.

Hijmans RJ, Karney C, Williams E, et al. 2024(2024-10-04). geosphere: spherical trigonometry. https://cran.r-project.org/package=geosphere.

Johnson CN, Balmford A, Brook BW, et al. 2017. Biodiversity losses and conservation responses in the Anthropocene. *Science*, **356**(6335): 270–275.

Kartzinel TR, Chen PA, Coverdale TC, et al. 2015. DNA metabarcoding illuminates dietary niche partitioning by African large herbivores.

Proceedings of the National Academy of Sciences of the United States of America, **112**(26): 8019–8024.

Levine JM, HilleRisLambers J. 2009. The importance of niches for the maintenance of species diversity. *Nature*, **461**(7261): 254–257.

Li YG, Chen M, Gong JL, et al. 2019. Saving China's onager. *Science*, **363**(6428): 701.

Lopes CM, De Barba M, Boyer F, et al. 2015. DNA metabarcoding diet analysis for species with parapatric vs sympatric distribution: a case study on subterranean rodents. *Heredity*, **114**(5): 525–536.

MacArthur R, Levins R. 1967. The limiting similarity, convergence, and divergence of coexisting species. *The American Naturalist*, **101**(921): 377–385.

MacArthur RH, Pianka ER. 1966. On optimal use of a patchy environment. *The American Naturalist*, **100**(916): 603–609.

Matthews JK, Ridley A, Kaplin BA, et al. 2020. A comparison of fecal sampling and direct feeding observations for quantifying the diet of a frugivorous primate. *Current Zoology*, **66**(4): 333–343.

Milinski M. 1982. Optimal foraging: the influence of intraspecific competition on diet selection. *Behavioral Ecology and Sociobiology*, **11**(2): 109–115.

Oksanen J, Kindt R, Legendre P, et al. 2007. The vegan package. *Community Ecology Package*, **10**(719): 631–637.

Pansu J, Guyton JA, Potter AB, et al. 2019. Trophic ecology of large herbivores in a reassembling African ecosystem. *Journal of Ecology*, **107**(3): 1355–1376.

Pansu J, Hutchinson MC, Michael Anderson T, et al. 2022. The generality of cryptic dietary niche differences in diverse large-herbivore assemblages. *Proceedings of the National Academy of Sciences of the United States of America*, **119**(35): e2204400119.

Perry G, Pianka ER. 1997. Animal foraging: past, present and future. *Trends in Ecology & Evolution*, **12**(9): 360–364.

Pfennig DW, Pfennig KS. 2010. Character displacement and the origins of diversity. *The American Naturalist*, **176**(S1): S26–S44.

Pringle RM, Kartzinel TR, Palmer TM, et al. 2019. Predator-induced collapse of niche structure and species coexistence. *Nature*, **570**(7759): 58–64.

R Core Team. 2025. R: a language and environment for statistical computing. https://www.r-project.org/.

Schoener TW. 1974. Resource partitioning in ecological communities. *Science*, **185**(4145): 27–39.

Shao XN, Lu Q, Xiong MY, et al. 2021. Prey partitioning and livestock consumption in the world's richest large carnivore assemblage. *Current Biology*, **31**(22): 4887–4897. e5.

Shipley LA, Forbey JS, Moore BD. 2009. Revisiting the dietary niche: when is a mammalian herbivore a specialist?. *Integrative and Comparative Biology*, **49**(3): 274–290.

Stewart DRM. 1967. Analysis of plant epidermis in faeces: a technique for studying the food preferences of grazing herbivores. *Journal of Applied Ecology*, **4**(1): 83–111.

Storr GM. 1961. Microscopic analysis of faeces, a technique for ascertaining the diet of herbivorous, mammals. *Australian Journal of Biological Sciences*, **14**(1): 157–164.

Sun W. 2024(2024-06-26). Dataset of desert plant list in Xinjiang. Science Data Bank. https://doi.org/10.57760/sciencedb.j00001.00791.

Taberlet P, Coissac E, Pompanon F, et al. 2007. Power and limitations of the chloroplast t*rn* L (UAA) intron for plant DNA barcoding. *Nucleic Acids Research*, **35**(3): e14.

Turghan MA, Jiang ZG, Niu ZZ. 2022. An update on status and conservation of the Przewalski's horse (*Equus ferus przewalskii*): captive breeding and reintroduction projects. *Animals*, **12**(22): 3158.

Valentini A, Miquel C, Nawaz MA, et al. 2009. New perspectives in diet analysis based on DNA barcoding and parallel pyrosequencing: the *trn*L approach. *Molecular Ecology Resources*, **9**(1): 51–60.

Van Driessche JA, Chamaillé-Jammes S, Nutter CM, et al. 2025. Water economics of African savanna herbivores: how much does plant moisture matter?. *Journal of Animal Ecology*, **94**(4): 670–681.

Vogel JT, Somers MJ, Venter JA. 2019. Niche overlap and dietary resource partitioning in an African large carnivore guild. *Journal of Zoology*, **309**(3): 212–223.

Westoby M, Rost GR, Weis JA. 1976. Problems with estimating herbivore diets by microscopically identifying plant fragments from stomachs. *Journal of Mammalogy*, **57**(1): 167–172.

Wickham H. 2016. Ggplot2: Elegant Graphics for Data Analysis. 2nd ed. Cham: Springer.

Willerslev E, Davison J, Moora M, et al. 2014. Fifty thousand years of Arctic vegetation and megafaunal diet. *Nature*, **506**(7486): 47–51.

Xia CJ, Cao J, Zhang HF, et al. 2014. Reintroduction of Przewalski's horse (*Equus ferus przewalskii*) in Xinjiang, China: the status and experience. *Biological Conservation*, **177**: 142–147.

Xu WX, Liu W, Ma W, et al. 2022. Current status and future challenges for khulan (*Equus hemionus*) conservation in China. *Global Ecology and Conservation*, **37**: e02156.

Xu WX, Yang WK, Zhang C, et al. 2016. Main plant communities and characteristics of Kalamaili Ungulate Nature Reserve in east Junggar Basin. *Chinese Journal of Plant Ecology*, **40**(5): 502–507. (in Chinese)

Zhang JL. 2025(2025-01-08). Spaa: SPecies association analysis. https://cran.r-project.org/package=spaa.

Zhu D, Wu F, Li HL, et al. 2023. Diet preferences based on sequence read count: the role of species interaction in tissue bias correction. *Molecular Ecology Resources*, **23**(1): 159–173.